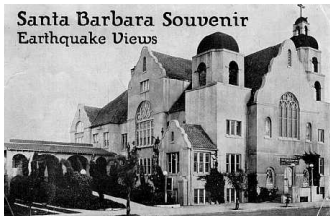

4th IASPEI / IAEE International Symposium:

Effects of Surface Geology on Seismic Motion

August 23–26, 2011 · University of California Santa Barbara

EFFECT OF SHORELINE FAULT ZONE SEGMENTATIONS ON SIMULATION OF LONG-PERIOD SEISMIC MOTIONS AND SEISMIC LOAD FOR DIABLO CANYON POWER PLANT

Dr. Alexander BYKOVTSEV
Regional Academy of Natural Sciences,
2644 Foghorn Cove, Port Hueneme, CA 93041,
USA, e-mail: bykovtsev1@yahoo.com

Marat KASIMOV
Regional Academy of Natural Sciences,
Port Hueneme, CA 93041,
USA, e-mail: manmarkaz@mail.ru

ABSTRACT

Effect of Shoreline fault zone (SFZ) segmentations on simulation of long-period seismic motions (LPSM) and seismic load will be presented for Diablo Canyon Power Plant (DCPP). The SFZ located about 1km offshore of DCPP and divided into three segments (North, Central, and South) based on differences in the geologic expression of surface and near-surface faulting. The Central segment of the SFZ is located 300 meters southwest of the Intake structure and 600 meters southwest of the Power Block. Although the initial seismic sensitivity studies showed that DCPP has adequate margin to withstand ground motion from the potential SFZ, both US Nuclear Regulatory Commission (NRC) and Pacific Gas and Electric (PG&E) recognized the need to better constrain the four main parameters of the SFZ needed for a seismic hazard assessment (SHA): fault geometry (length, dip, down-dip width), segmentation, distance offshore from DCPP, and slip-rate. To address some of this need, we conducted numerical calculations to analyze and interpret the effect of SFZ segmentations on LPSM. The methodology for synthesizing LPSM based on 3D-analytical solutions by Bykovtsev-Kramarovskii (1987&1989) constructed for faults with multiple segmentations. This approach is based on a kinematics description of displacement function on the fault, included in consideration of all possible combinations of 3 components of vector displacement (two slip vectors and one tension component) and provided more accurate LPSM evaluations. From our preliminary calculation (Bykovtsev 2011) it was discovered that for DCPP site LPSM might contain pulses with multiple oscillations (due to SFZ segmentation), which can cause severe nonlinear structural response. LPSM with multiple oscillations have become a crucial consideration in SHA of DCPP. These findings shall be investigated more fully.

INTRODUCTION

The focus of work is on the prediction of long-period seismic motions (LPSM) and seismic load from seismic sources for Diablo Canyon Power Plant (DCPP) area located near the Shoreline Fault Zone (SFZ) in Central Coastal California. Here LPSM refers to all aspects of a seismogram including ground displacements, velocities, accelerations, and duration of motion. The effect of SFZ segmentations on simulation of LPSM and seismic load will be investigated for DCPP according to NRC Regulations and new requirements of American Society of Civil Engineers Standard (ASCE 7-10 Chapter 21 Site-Specific Ground Motion Procedures for Seismic Design). Practical application of the ASCE 7-10 (Chapter 21) contains new and significantly revised procedures for site-specific ground motions for building code applications. According to new requirements of the (ASCE 7-10) at least five recorded or simulated horizontal ground motion acceleration time histories shall be selected from events having magnitudes and fault distances that are consistent with those that control the Maximum Considered Earthquake (MCE). For some cases (e.g. from M6.0 to M8, less than 5 km from the fault zone), there may not be five sets of recorded ground motions that are appropriate and simulated ground motion would be needed. Based on analytical and numerical simulation for the earthquake rupture propagations ground-motion modeling methods are being increasingly used to supplement the recorded ground-motion database. Unfortunately, there is no official procedure to follow for near-field sites (D < 5 km from the fault). This presents a paradox: the Building Codes and Standard ASCE/SEI 7-10 requires engineers to provide simulation of ground motion records (Chapter 21), but there is no official procedure for accomplishing this at near-field sites. This paradox should be resolved as soon as possible.

Investigation and prediction of the strong ground motion near an earthquake source are some of the most important tasks of engineering seismology. There is no doubt that the peculiarities of the peak amplitudes, duration and frequency content of the near-field motion, which are caused by the features of the earthquake source rupture process, may strongly influence the damage distribution in the epicenter zone. Traditionally, the studies in the field of near-source motion were focused on high-frequency (from 0.8-1.0 to 15-20 Hz) motion. The recent large earthquakes in Japan, Spain, Turkey, Taiwan, and California reveal the importance of low-frequency (less than 0.7-0.3 Hz) radiation that is now considered as one of the characteristic properties of the near-field strong ground motion. Also, one of the most important achievements in understanding the earthquake source nature is the evidence of the complex non-planar form of the main fault with several twisting segments. Consequently, when analyzing the seismic radiation from a large earthquake source within the broad frequency range, it is necessary to consider both the discrete character of the source properties (heterogeneous rupture processes and dislocation distribution along the fault) controlling the high-frequency radiation and the geometrical characteristics (configuration and dimensions of the main fault and sub-faults) of the source and properties of the rupture propagation medium. The numerical simulation of the dynamic heterogeneous rupture propagation along curvilinear (twisting) and branching trajectories (Bykovtsev A.S 1986a,b) may be considered as a powerful tool for studying the complex source zones and understanding the physical nature of an earthquake source. Development of 3D models and deterministic simulation of spontaneous rupture propagation (Bykovtsev and Kramarovskii, 1986, 1987, 1989), that take account of additional complexity in fault geometry including multiple fault segmentation and non-planar faults models, allow us to predict and analyze the maximum probable ground motion parameters in the near zone of MCE more accurate and in a precise manner.

The SFZ located about 1km offshore of DCPP and divided into three segments (North, Central, and South) based on differences in the geologic expression of surface and near-surface faulting. The Central segment of the SFZ is located 300 meters southwest of the Intake structure and 600 meters southwest of the Power Block. Although the initial seismic sensitivity studies showed that DCPP has adequate margin to withstand ground motion from the potential SFZ, both US Nuclear Regulatory Commission (NRC) and Pacific Gas and Electric (PG&E) recognized the need to better constrain the four main parameters of the SFZ needed for a seismic hazard assessment (SHA): fault geometry (length, dip, down-dip width), segmentation, distance offshore from DCPP, and slip-rate. To address some of this need, we conducted numerical calculations to analyze and interpret the effect of SFZ segmentations on LPSM. From our preliminary calculations (Bykovtsev 2011) it was discovered that for DCPP site LPSM may contain cyclic load and pulses with multiple oscillations (due to SFZ segmentation) which can cause severe nonlinear structural response. LPSM with multiple oscillations have become a crucial consideration in SHA of DCPP due to cyclic load, which may cause a type of crack called a "fatigue crack" in structure. The nature of such cyclic loading induces progressive alteration in the bearing capacity and head displacement of the foundation. This may sometimes lead to disastrous consequences (Japan-March 2011 lessons). These findings shall be investigated more accurate for seismic hazard assessment.

SITE DESCRIPTION

The DCPP site with intensive previous geotechnical investigations was selected for development and demonstrations new methodologies and procedures obtaining LPSM records for planar and non-planar fault topology within 5 km of a SFZ. The site geographic coordinates are 35.211° north latitude and -120.8544° west longitude. Coordinate for SFZ segments and DCCP are presented in Figure 1 and Table 1. The site was previously investigated by PG&E in 1990-2011. The PG&E (2011) report presents the results of a two-year PG&E study of the SFZ, which is located offshore of the DCPP. In November 2008, PG&E informed the NRC that preliminary results from the DCPP Long Term Seismic Program seismic hazard update showed an alignment of seismicity that suggested the presence of a previously unidentified fault approximately 1 kilometer (km) offshore of DCPP. This previously unidentified fault was subsequently named the Shoreline Fault Zone (SFZ) by PG&E. The SFZ is located along the coastal margin of the San Luis Range in south-central California near San Luis Obispo. This region of California is characterized by transpressional deformation between the San Andreas Fault zone to the east and the San Gregorio–San Simeon–Hosgri system of near-coastal faults to the west (Fig. 1). The SFZ is conservatively assumed to be up to 23 km long and has an overall strike of N60' W to N70' W.

The DCPP is located on the southwestern slope of the Irish Hills (Fig. 1) in the northern part of the San Luis Range, a prominent west-northwest-trending topographic and structural high that forms the core of one of the more prominent uplifted structural blocks (the San Luis–Pismo block) in the Los Osos domain PG&E (2011). The topographic relief on the site ranges from about elevation 300 feet near the road above DCCP to 50 feet near the toe of the slope, producing a slope gradient of about 2.5:1 (horizontal: vertical), i.e., approximately 22 degrees. The range is uplifting as a relatively rigid crustal block bordered by the northwest-trending Los Osos and

Southwestern Boundary zone faults. Elevations and ages of the marine terraces on the southwest side of the San Luis Range show that the range is uplifting at rates of between 0.1 mm/yr to the southeast to 0.2 mm/yr to the northwest, with little or no observable internal deformation. According to PG&E (2011) report, major geologic structures within the range, including the Pismo syncline, which cores the Irish Hills, and the San Miguelito, Edna, and Pismo faults, do not deform Quaternary deposits or landforms and are not active structures in the contemporary tectonic setting. Previously characterized active fault zones bordering the San Luis–Pismo block to the northeast, southwest, and west are the Los Osos, Southwestern Boundary (including the San Luis Bay fault zone), and Hosgri fault zones, respectively (Fig. 1).

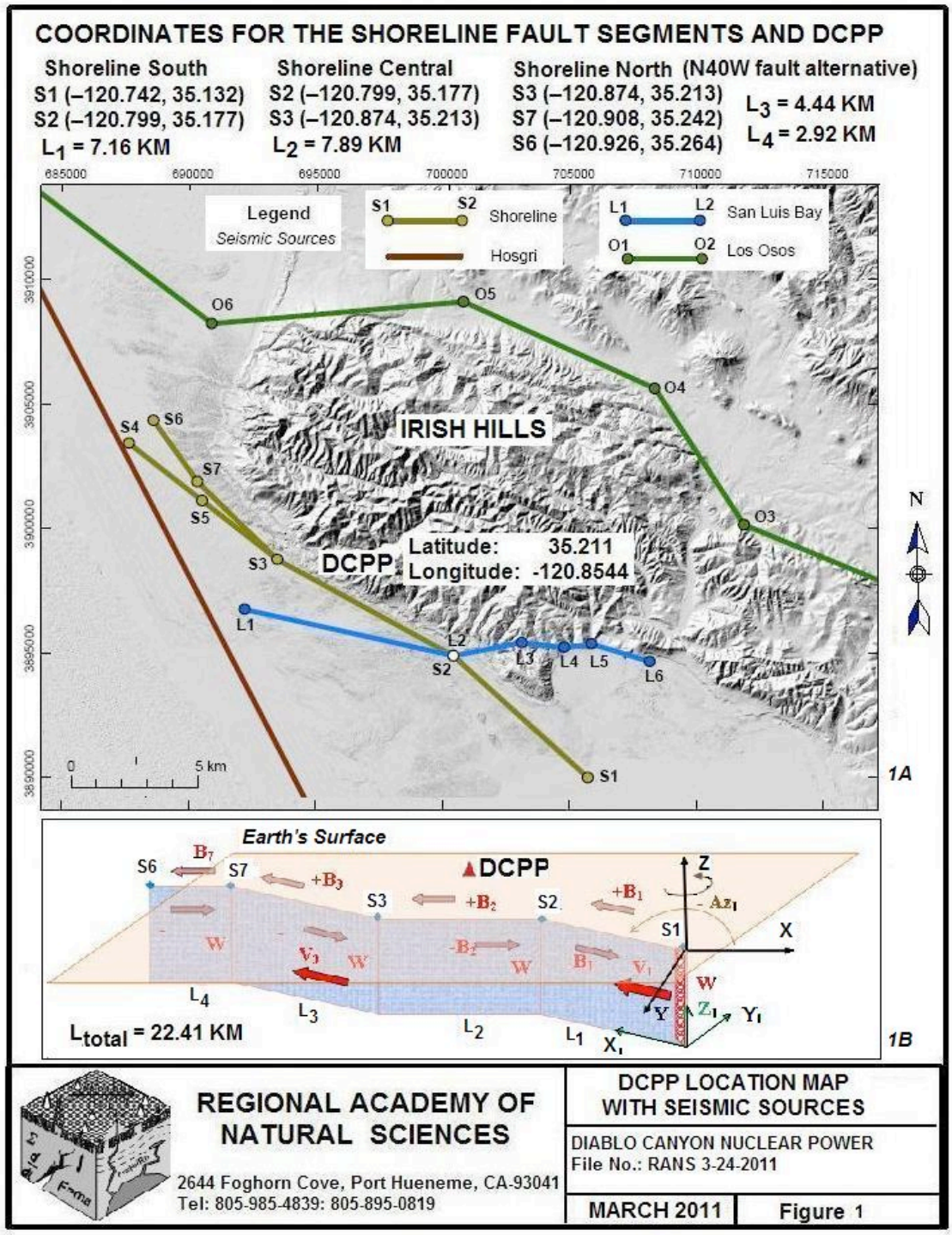

Fig. 1. DCPP Location Map with seismic sources (1A) and coordinates systems locations (1B)

Table 1. Coordinates for the Shoreline Fault segments and DCPP.

COORDINATES FOR THE SHORELINE FAULT SEGMENTS AND DCPP			
South Segment	**Central Segment**	**North Segment** (S4 end point alternative)	**North Segment** (N40W fault alternative)
S1 (–120.742, 35.132)	S2 (–120.799, 35.177)	S3 (–120.874, 35.213)	S3 (–120.874, 35.213)
S2 (–120.799, 35.177)	S3 (–120.874, 35.213)	S5 (–120.906, 35.235) S4 (–120.937, 35.256)	S7 (–120.908, 35.242) S6 (–120.926, 35.264)
Length Ls_{1-2}=7.16 km	Length Ls_{2-3}=7.89 km	Length Ls_{3-5}=3.78 km Length Ls_{5-4}=3.64 km	Length Ls_{3-7}=4.44 km Length Ls_{7-6}=2.92 km
DCPP – Latitude: 35.211; Longitude -120.8544; Length Ls_{1-DCPP}=13.41 km			

The faulting style of SFZ is inferred to be primarily a right-lateral fault based on focal mechanisms that indicate **vertical strike-slip fault motion** and the linear geologic expression of the fault on the seafloor along the Central and South segments PG&E (2011). However, some focal mechanisms along the North and Central segments show **right-oblique or right-reverse motion**, and one focal mechanism along the South segment shows right-normal motion. These oblique mechanisms suggest that the fault may accommodate some **vertical displacement** as well as **lateral displacement**. However, as discussed in Section 4.4 PG&E (2011), the vertical component of displacement along the Shoreline fault zone is less than approximately 2 m on submerged wavecut platforms estimated to be 75,000 years old or older. These data support a characterization of the SFZ as a **strike-slip fault with a limited vertical component.**

The northeastern margin of the San Luis Range is bordered by the **Los Osos fault zone**, which separates the uplifting range from the subsiding or southwest-tilting Cambria block to the northeast. The Los Osos fault zone has had a complex history of both **strike-slip and dip-slip** displacement (Lettis and Hall, 1994). The fault zone is a 50 km long, 2 km wide system of discontinuous, subparallel, and en echelon fault traces extending from Estero Bay on the north to an intersection with the West Huasna fault southeast of San Luis Obispo. Along the coast, the fault zone truncates a flight of marine terraces, indicating a **vertical rate of separation across the fault zone** of about 0.2 mm/yr. Preliminary results from new geomorphic mapping, interpretation of reprocessed seismic-reflection data, analysis of seismicity data, and structural analysis suggest that the fault zone dips steeply to the southeast (45 to 70 degrees or possibly steeper), and may be primarily an **oblique-slip fault**, with a **significant component of dip slip** to accommodate uplift of the range.

The **Hosgri and San Simeon fault zones** are characterized by 1–3 millimeters per year (mm/yr) of **right-lateral slip**, with the rate of slip increasing from south to north along the San Gregorio–San Simeon–Hosgri fault system, ultimately to 6–8 mm/yr on the San Gregorio fault zone to the north in the San Francisco Bay area PG&E (2011). Whereas the Hosgri fault zone is offshore for its total length, the San Simeon fault zone is onshore between Ragged Point and San Simeon Point for part of its length. Focal mechanisms and the distribution of seismicity along the Hosgri fault zone document nearly pure strike-slip on a near-vertical to steeply east-dipping fault to a depth of 12 km (McLaren and Savage, 2001; Hardebeck, 2010). The Hosgri fault zone is the southern portion of the larger 410 km long San Gregorio–San Simeon–Hosgri fault system. It is an active transpressional, convergent **right-slip fault zone** that extends southeastward approximately 110 km from a location 6 km offshore of Cambria to a point 5 km northwest of Point Pedernales (Hanson et al., 2004).

The **San Luis Bay Fault Zone** within the Southwestern Boundary fault zone, the San Luis Bay fault zone lies closest to the DCPP. The general location of the fault zone is well constrained onshore but is less well constrained offshore both to the east in San Luis Obispo Bay and to the west toward the Hosgri fault zone. Onshore a strand of the fault zone is exposed along Avila Beach Road, where it juxtaposes Franciscan basement over the Squire Member of the Pismo Formation and displaces an overlying marine wave-cut platform and associated marine terrace deposits (see PG&E (2011) report). A fault strand also displaces fluvial deposits at the mouth of San Luis Obispo Creek before extending offshore to the east into San Luis Obispo Bay. Farther east, the fault zone is interpreted to extend to a location offshore of Mallagh Landing, where it either dies out or intersects the offshore projection of the San Miguelito fault. The fault zone does not extend onshore east of Mallagh Landing, confirming that this is the eastern end of the fault zone. To the northwest of Avila Beach, the San Luis Bay fault zone crosses a topographic saddle north of Point San Luis where the fault is blind, but beneath the onshore coastal terraces the fault diverges into two distinct traces or zones that deform the marine terraces. The southern trace is named the Rattlesnake fault and has a **vertical separation rate** of about 0.08 mm/yr. The northern trace is named the Olson Hill deformation zone in PG&E (2011). The Olson Hill deformation zone appears to form a monoclinal bend in the marine terraces with a **total vertical separation** of about 0.06 mm/yr. The cumulative **rate of vertical separation** across these two parts of the San Luis Bay fault zone along the external coast is about 0.14 mm/yr. Offshore to the west, the fault zone is interpreted to extend either to an intersection with the Shoreline fault zone (for a total fault length of 8 km) or across the Shoreline fault zone to an intersection with the Hosgri fault zone (for a total fault length of 16 km).
The detailed descriptions of the seismic characteristics of the Shoreline fault zone were developed from extensive geologic,

geophysical, and seismological databases and accurately presented in PG&E Reports (2010, 2011).

Based on the recommendations presented in the Report on the analysis of the Shoreline Fault Zone, Central Coastal California, prepared by PG&E Report to the NRC and dated January, 2011, additional investigation and analyses were determined to be needed for characterization of those seismic sources and ground motions most important to the DCPP: the Hosgri, Shoeline, Los Osos and San Luis Bay faults zones and other faults within the Southwestern Boundary zone. Although the initial seismic sensitivity studies showed that DCPP has adequate margin to withstand ground motion from the potential SFZ, both NRC and PG&E recognized the need to better constrain the four main parameters of the SFZ needed for a seismic hazard assessment (SHA): fault geometry (length, dip, down-dip width), segmentation, distance offshore from DCPP, and slip-rate.

In addition, it should be noted that the report "Diablo Canyon, Units 1 and 2, Report on the Analysis of the Shoreline Fault Zone, Central Coastal California, Chapter 6.0 - Seismic Hazard Analysis - Appendix A-3" did not comply with NRC Regulatory Guidance.
According to NRC Regulations Title 10, Code of Federal Regulations in § 100.23 Geologic and seismic siting criteria it is clear stated: (1) Determination of the Safe Shutdown Earthquake Ground Motion. The Safe Shutdown Earthquake Ground Motion for the site is characterized by **both horizontal and vertical free-field ground motion** response spectra at the free ground surface. In PG&E (2011) report the estimation was done only for horizontal peak ground acceleration (PGA). This Safe Shutdown Earthquake Ground Motion has a horizontal PGA of 0.75 g based on the assumption of a magnitude 7.5 earthquake on the Hosgri Fault, which is located 5 km (3 mi) from the DCPP. Unfortunately, Vertical component of ground motion was not included in consideration in PG&E Report (2011) and did not comply with NRC Regulatory Guidance. (See also requirements from Regulatory Guide 1.92 – Combining modal responses and spatial components in seismic response analysis.) Only horizontal ground motion was included in the PG&E (2011) report, with the vertical component being eliminated from consideration. However, it was clear publicized that the vertical component, especially for dip movement in the fault, will be responsible for maximum velocity and peak ground acceleration. The publication "The Slapdown Phase in High-acceleration Records of Large Earthquakes" by Masumi Yamada, Jim Mori, and Thomas Heaton in *Seismological Research Letters* Volume 80, Number 4, July/August 2009, presented a list of the records in which the vertical acceleration exceeds 1,000 cm/s^2 (>1g). The vertical component of ground-motion acceleration, at least for dip-slip-oriented movement on the SFZ (reverse and normal faults), should be included in Site-Specific Ground Motion Procedures for proper seismic hazard assessment DCPP.
Also, in § 100.23 Geologic and seismic siting criteria it is clear stated: (4) Determination of siting factors for other design conditions. Siting factors for other design conditions that must be evaluated include soil and rock stability, liquefaction potential, natural and artificial slope stability, cooling water supply, and remote safety-related structure siting. Each applicant shall evaluate all siting factors and potential causes of failure, such as, the physical properties of the materials underlying the site, ground disruption, and the effects of vibratory ground motion that may affect the design and operation of the proposed nuclear power plant. In the case where a causative fault is near the site, the effect of proximity of an earthquake on the spectral characteristics of the Safe Shutdown Earthquake shall be taken into account. The effects of vibratory ground motion, due to faults segmentation (See A.S. Bykovtsev's publications 1979-2011) also were not included in consideration in PG&E Report (2011).

TECHNICAL APPROACH FOR SEISMIC MOTION SIMULATION PROCEDURE.

According to the new requirements of the ASCE Standard (ASCE/SEI 7-10 Chapter 21 Site-Specific Ground Motion Procedures (SSGMP) for Seismic Design) at least five recorded or simulated ground motion (SGM) time histories shall be selected from events having magnitudes and fault distances that are consistent with those that control the Maximum Considered Earthquake (MCE). In mean time there are not enough recorded ground motions especially in the near-field of large earthquakes with magnitudes Mw>6 at the distances less than 5 km from the fault, and deterministic simulated ground motion (DSGM) would be needed for proper Seismic Hazard Analysis DCPP.

According to ASCE 7-10 Chapter 21, probabilistic and deterministic MCE analyses are now mandatory included in SSGMP. The Probabilistic Seismic Hazard Analysis (PSHA) was conducted to evaluate the likelihood of future earthquakes and provide design ground motions. The PSHA based on IBC-2006 and ASCE/SEI 7-05 provides very limited results, and not valid for near zone due to absent of real seismic data for structure located close to the fault (inside 1km zone). Also, within the limit of PSHA, the effects of vibratory ground motion that may affect the design and operation of the proposed nuclear power plant due to cyclic load were not included in consideration.

For structural nonlinear analyses, it is desirable to have additional time histories because of the importance of information about cyclic load phasing, pulses sequencing and their amplitudes to nonlinear response. In the past, when using selected recorded motions, simple scaling of acceleration time histories was frequently performed to enhance spectral fit. The results of significant scaling of acceleration time-histories on velocity, displacement, and energy can be profound. Relation horizontal to vertical components are very sensitive to faulting style and it is not appropriate to use the procedure, when the same simple scaling factors are applied to the other

horizontal components and the vertical components for the records selected, the spectral fit is usually not as good for the other components. We not recommended using in the future scaling approach for DCPP due to differences in fault segmentations for different faults and sites locations.

Simulated seismic sources time histories and time-domain procedures are one of more effective method that may be used for proper estimate the effects of vibratory ground motion and several cyclic load on DCPP foundation and non-structural elements.

The Deterministic Seismic Hazard Analysis (DSHA), including fault segmentation, will be used for control and correction of results obtained by PSHA screening procedures. Our expectation is that DSHA will provide more accurate results in near-fault zones and more realistic results for slope stability analyses with time history analysis procedures for DSGM. The results of a quantitative Site-Specific Seismic Investigation (SSSI) based on DSGM under ASCE/SEI-7-10 will be presented for strike-slip fault movement and for different scenarios seismic sources inside SFZ. The lack of manuals for deterministic simulated ground motion (DSGM) analyses with clear description of existing approaches stimulated us (Bykovtsev 2009a,b,c) to provide analyses and review main priorities and limitations (including advantages and disadvantages) of existing methods for DSGM from the practical point of view of their application to the geotechnical industry.

The purpose of this SSSI study will be to satisfy the NRC and PG&E comments and provide preliminary conceptual geotechnical recommendations, methodologies and procedures for DSGM from planar and non-planar (twisted) faults topology within 5 km of a fault zone with multiple segmentations. Usually, LPSM computed based on kinematic rupture representations consistent with seismic, geodetic, and geologic observations and using analytical algorithm Bykovtsev-Kramarovskii-1987. LPSM were computed for planar and non-planar (twisted) fault topology and presented in Fig.2-5 for four different scenarios of seismic sources in SFZ as results of SSSI.

We will use Boundary Element Method (BEM) and Bykovtsev's models to produce LPSM for DCPP area. In Bykovtsev-Kramarovskii (1987 &1989) publications an **exact analytic solution** was constructed for the non-stationary 3D- problem of the propagation of a rectangular fracture area on which a **complex fracture process** was given (two shear components with tension or opening component). Both scenarios were considered for fracture area starting at subsonic and supersonic speed on which a complex fracture process (shear components with tension or opening component) was given. To describe the fracture process occurring at the complex rupture plane, a kinematic approach was used for which the magnitude and direction of the dislocation vector on the each flat segment of rupture plane were given on the whole fracture area as a Boundary Conditions. For details see publications (Bykovtsev A.S 1986a,b), (Bykovtsev and Kramarovskii, 1986, 1987, 1989). At the present time research efforts in the area of theoretical modeling of fracture processes occurring in focal zones of tectonic earthquakes are directed towards the production of those models (describing the ripping open processes at a focus), which would allow a description of the singularities of high-frequency radiations in the best manner. In (Bykovtsev and Sokolov, 1989&1990) publications peculiarity of high-frequency radiations in the near zone of the faults with multiple segmentations were considered.

BEM Model developed by Dr.Bykovtsev represents the LPSM time history simulation procedure, constructed for the single rectangular flat fault and for faults with multiple segments using computer codes developed by Bykovtev and Kasimov (1989-2011), and based on 3D-analytical solutions published by Bykovtsev-Kramarovskii (1987&1989). Comprehensive computer codes were initially written in the FORTRAN and rewritten on algorithmic language Visual C # 2008, which most to be suitable for describing structural data also on the base to the platform of v.3.5.NET Framework not required tuning of operating system. The interface of input-output is English and Russian. Program is compact (it does not require the large volumes of working storage) and is high speed. Our computer codes provide possibility sufficiently easily and rapidly (in 15-20 seconds with the prepared templates) to build the models of the seismic sources of any complexity with 200-300 fault trajectories and up to 50 sub-segments on each fault. This procedure is based on a kinematic description of the displacement function on the fault and includes in consideration all possible combinations of 3 components of vector displacement (two slip vectors and one tension or opening component). The opportunity to take into consideration both shear and open vector components of displacement, radiation patterns and directivity effects will open new future possibilities for decreasing the number of epistemic uncertainty in seismic hazard studies. It will supply as more accurate and more physically realistic results for simulated ground motion, computing slope stability and dynamic soil pressures and structural response of deeply embedded structures. The model also provides the opportunity to evaluate wide frequency diapasons for jump-like rupture break-up and rupture movement along curvilinear and non-planar (twisted) trajectories due to real fault segmentations. This algorithm is perfect for near- middle- and far-field distances from the fault. This approach competes with both widely used Stochastic Point-Source and Finite-Fault Models and includes stable source mechanism parameters and fault segmentations in consideration through computing time histories of strong ground motion for large earthquakes, different Seismic Load Conditions (SLC) and different combinations of vertical-to-horizontal load ratios as functions of magnitude, distance, **source mechanism** and **fault segmentations**. The Bykovtsev' Model was widely used for accurate description of rupture processes in solid materials for different geotechnical project in Russia, Uzbekistan and California.
Because all models are mathematical approximations to complicated real physical fracture processes occurring as a result of seismic events, rigorous verification and validation exercises are necessary to evaluate model accuracy and set up the boundaries for parameter

values and their uncertainties. It is clear that due to the absence of records for DCPP conditions, methodical verification and validation exercises to judge model accuracy and parameter distributions will be very difficult. Several verification and validation tests for computer codes based on Bykovtsev (1986 a,b) and Bykovtsev-Kramarovskii (1987&1989) algorithms were done by Dr. Vladimir Graizer (now a seismologist in U.S. Nuclear Regulatory Commission) at the Institute of Earth Physics (Moscow, Russia). It was documented that comparing Bykovtsev's procedure with alternative numerical procedures for Finite-Fault Model based on Green's functions solution provided identical results, but the time of calculation was reduced by 3,000 times in comparison with numerical procedures based on Green's functions solution. Additionally, M. Kasimov modified the algorithm and achieved a 3.5 times speed improvement of the Bykovtsev-Kramarovskii algoritm (1987). Ultimately, it was documented that Bykovtsev-Kramarovskii (1987&1989) algorithm with Kasimov's modifications (Bykovtsev and Kasimov 2009) is 10,000 times faster than numerical algorithms based on Green's functions. After official validation tests (protocol of comparison DSGM with laboratory modeling and natural records available upon request), the computer codes were recommended by the USSR government for use in earthquake engineering and mining industries. A number of natural experiments in Norilsk Mining Group (Russia) during 1988-1992 and Navoi Gold Mining Group (Uzbekistan) during 1994-1999 with comparison DSGM and recorded ground motion were documented and published in book (Bykovtsev *et al*. [2000]). Additionally, the presented approach and methods have been quite successful in generating realistic DSGM compared with observations for earthquakes and explosions, and has been applied to many DSGM geotechnical engineering and mining projects (Bykovtsev *et al*. [2000]). In 1995 the Bykovtsev's procedure and approach with DSGM for a maximum considerable earthquake with M=6.5 in Tashkent (Capital of Uzbekistan) was successfully used for site specific seismic investigation by the Uzbek Government for design and construction of the multi-level (22-story) National Bank and National Gold Repository of Uzbekistan. The site is located inside the intersection of three active faults and approximately within 2km zone from the epicenter of the catastrophic Tashkent-1966 earthquake M=5.3. Natural seismo-records from the Tashkent-1966 and Nazarbek-1980 earthquakes were used to navigate a mathematical model and generated DSGM for structural deign (Bykovtsev and Kasimov 2009).

In Bykovtsev's (2009a,b,c) SSA-2009 presentations a comparison of empirical PGA attenuation relations by Graizer-Kalkan-2007 and simulated horizontal PGA for strike-slip were provided. For the Parkfield Earthquake of 9/28/04 with M=6.0 it was clearly demonstrated that compared results of simulated PGA and empirical PGA versus Distance are similar and in good correlation for different distances. It was shown that amplitude of ground motion definitely amplifies and exceeds 1.0g for R<300m from the fault. Additionally, it was discovered that DSGM provides local minimum (dip) with PGA approximately equal 0.16g for distance R=2±1km and local maximum (bump) with PGA approximately equal 0.67g for distance R=4±1km. For distance more than 5 km simulated PGA attenuates with 1/R. This fact will affect seismically-induced lateral earth pressures on walls and floors of deeply embedded structures and should be taken in consideration during recommendations on the appropriate use of numerical tools in assessing seismic soil-structure interaction under different seismic load conditions (SLC).

The technical approach based on BEM model will provide an opportunity to include different types of fracture mechanisms in main seismic source characterizations and the real fault segmentation in their considerations. The Bykovtsev's methodology will be more practical for proper seismic design of essential facilities (located in the zone of less than 5 km from the fault) **where deterministic simulated ground motion records for displacement, velocity and acceleration are mandatory.** This approach will benefit the geotechnical industry with new tools and new results which will be very helpful for optimal solving the main open questions in the development of recommendations for calculating soil pressures and structural response of partially to fully embedded structure under different SLC. However, the approach based on application BEM Model and Bykovtsev's methodology was previously published in top level rated peer-reviewed Russian journals with English translation and widely used by the government of Russia and Uzbekistan for design essential facilities. Several geotechnical projects were done in California.

To develop distance dependence approach to modeling seismic soil structure interaction for deeply embedded structures and to provide estimates for different material constitutive models for soil and/or structure under different SLC and different combinations of vertical-to-horizontal load ratios as functions of magnitude, distance, **source mechanism** and **fault segmentations** we will recommend using BEM Model and Bykovtsev's methodology and his procedure for DSGM. This procedure can be easily implemented on the SCEC/USGS Platform in the separate modules with specified input and output parameter types and formats, to provide for interchangeability between different procedures, and then be used to simulate ground motions that will contribute to the database for predicting and calculating seismically-induced lateral soil pressures and structural response of partially to fully embedded structures and other essential facilities under different seismic loading conditions.

SOURCES AND PROPAGATION MODELS

In this work we used the four main segments Shoreline Fault geometry that simulated four different seismic scenarios from different rupture models of SFZ. We calculated the synthetic LPSM at the DCPP and 100 meters below free surface. The simulations results for LPSM are presented on Fig. 2-5 for four different models. Here, for example, we show the results for the uniform and non-uniform slip distributions on Fig.2 and Fig.3 respectively. Fig. 2 illustrates input data, fault configuration and three-component results of LPSM for Shoreline Fault presented as one segment S1-S4 with strike angle -142.6^0 to axes OX, and uniform slip movement Bx=95cm. The Fig. 3 illustrates input data, fault configuration and three-component results of LPSM for Shoreline Fault presented as one segment S1-S4 with strike angle -142.6^0 to axes OX, and non-uniform (variable) slip movement Bx. The first segment S1-S2 split for 5 sub-segments and we assumed that for a rise time of 0.8 second average displacement on first segment reached 50 cm and then remain constant on first segment (Fig. 3), on the second segment S2-S3 average displacement jump up to 150 cm, and on third S3-S5 an fourth segment S5-S4 average displacement drop up to 100cm and 87 cm, respectively.

On Fig. 4 and 5 presented results for two different scenarios of bending SFZ and branching SFZ. The Fig. 4 illustrates input data, fault configuration and three-component results of LPSM for Shoreline Fault presented as four segments S1-S2, S2-S3, S3-S5, S5-S4 with non-uniform (variable) slip movement Bx as presented on Fig.3. Finally, the Fig. 5 illustrates input data, fault configuration and three-component results of LPSM for Shoreline Fault presented as six segments S1-S2, S2-S3, S3-S5, S5-S4, and branching segments S3-S7 and S7-S6 with non-uniform (variable) slip movement Bx. We assumed that for a rise time of 0.8 s average displacement on first segment reached 50 cm and then remain constant on first segment, on the second segment S2-S3 average displacement jump up to 150 cm, and on first branching third S3-S5 an fourth segment S5-S4 average displacement drop up to 50cm and 41 cm, respectively, and on second branching fifth segment S3-S7 and six segment S7-S6 average displacement drop up to 50cm and 46 cm, respectively. Real coordinates for segments S1-S2, S2-S3, S3-S5, S5-S4, S3-S7 and S7-S6 are presented in Table 1. Recalculated coordinates in global OXY coordinate system are presented in input data on Fig.4 and Fig.5. The strike angles for segments S1-S2, S2-S3, S3-S5, S5-S4, S3-S7 and S7-S6 are -136.6^0, -150^0, -140.43^0, -140.84^0, -134.3^0, -124.25^0, respectively.

We assumed a hard-rock, elastic velocity model with V_P and V_S equal to 6.0 km/s and 4 km/s, respectively. For all four models, in order to simulate motions for M_w 6.5 events, we used the relations of Leonard (2010) to determine the approximate length (23km) and width (15 km) of the Shoreline Fault. Given these dimensions an M_w 6.5 event has approximately 0.95 m of uniform slip over the SFZ. For all four models we assumed that rupture processes start in point S1 and moving in direction point S2, then to point S3, then to points S5 and S4a and in case branching scenario presented on Fig. 5 rupture movement occurs in two directions S5-S4 and S7-S6. We assumed that on all segments have constant ruptures velocities of 75% of the shear-wave velocity (V_S). A uniform-slip model presented on Fig.2 was used to examine simulated LPSM for SFZ and average estimation main parameters of LPSM for single segment strike-slip model and Fig. 3-5 show results for multiple fault segmentation effects. Location of basic coordinate systems and local coordinate systems are presented on Fig. 1B. It was estimated that maximum distance between DCPP and point S1 approximately equal $Ls_{1\text{-}DCPP}$=13.41 km. Also, for proper comparison all four different scenarios, we assumed that for all four models scalar seismic moment Mo=μ*B*L*W=Const= μ 0.32 (km), where μ- is shear modulus (Nkm^{-2}), B- is average fault displacement (cm), L- is fault rupture length (km), and W- is fault width (km). Only strike-slip (Bx≠0, By=0, Bz=0) cases were presented on Fig.2-5, but results may be easily recalculated with including more realistic dip-slip component (Bx≠0, By=0, Bz≠0) and tension component (Bx≠0, By≠0, Bz≠0) in consideration and analysis.

DISCUSSION AND RECOMMENDATIONS

The Uniform-slip Simulations for SFZ presented as a Single Segment S1-S4 with Strike Angle -142.6^0.

Two large amplitude pulse-like velocity ground motions on components X and Y, and one pulse-like velocity motion observed on vertical Z component Fig. 2 presents. Component X and component Y have a two strong maximum in acceleration and component Z has only one maximum in acceleration. As we can see from Fig.2 for the uniform-slip simulations the maximum differences between maximum and minimum peak ground velocity (PGV) and peak ground acceleration (PGA) values for Y components (81 cm/s and 1.13g, respectively), and for vertical Z component the maximum differences between maximum and minimum PGV and PGA (24.7 cm/s and 0.23g, respectively). The first PGA arrived at 3.38 sec and second PGA arriver at 4.46 sec and approximately 76% and 80% from first PGA for component X and component Y, respectively. Vertical motions in this case are approximately equal 30.5% to the horizontal component Y for velocities, and approximately 20.4% to the horizontal component Y for acceleration.

Recommendation # 1 for strike-slip with uniform movement on the SFZ. Based on obtained results for uniform-slip with average movement equal approximately 95 cm, for structural design DCPP foundation and nonstructural elements two seismic load with interval of action approximately 1.1 sec should be taken in consideration for proper Seismic Hazard Analysis. The total vector horizontal PGA for component X and Y for the first and second forces may be estimated around 1.5 g and 1.15 g, respectively, and vertical component Z around 0.23 g.

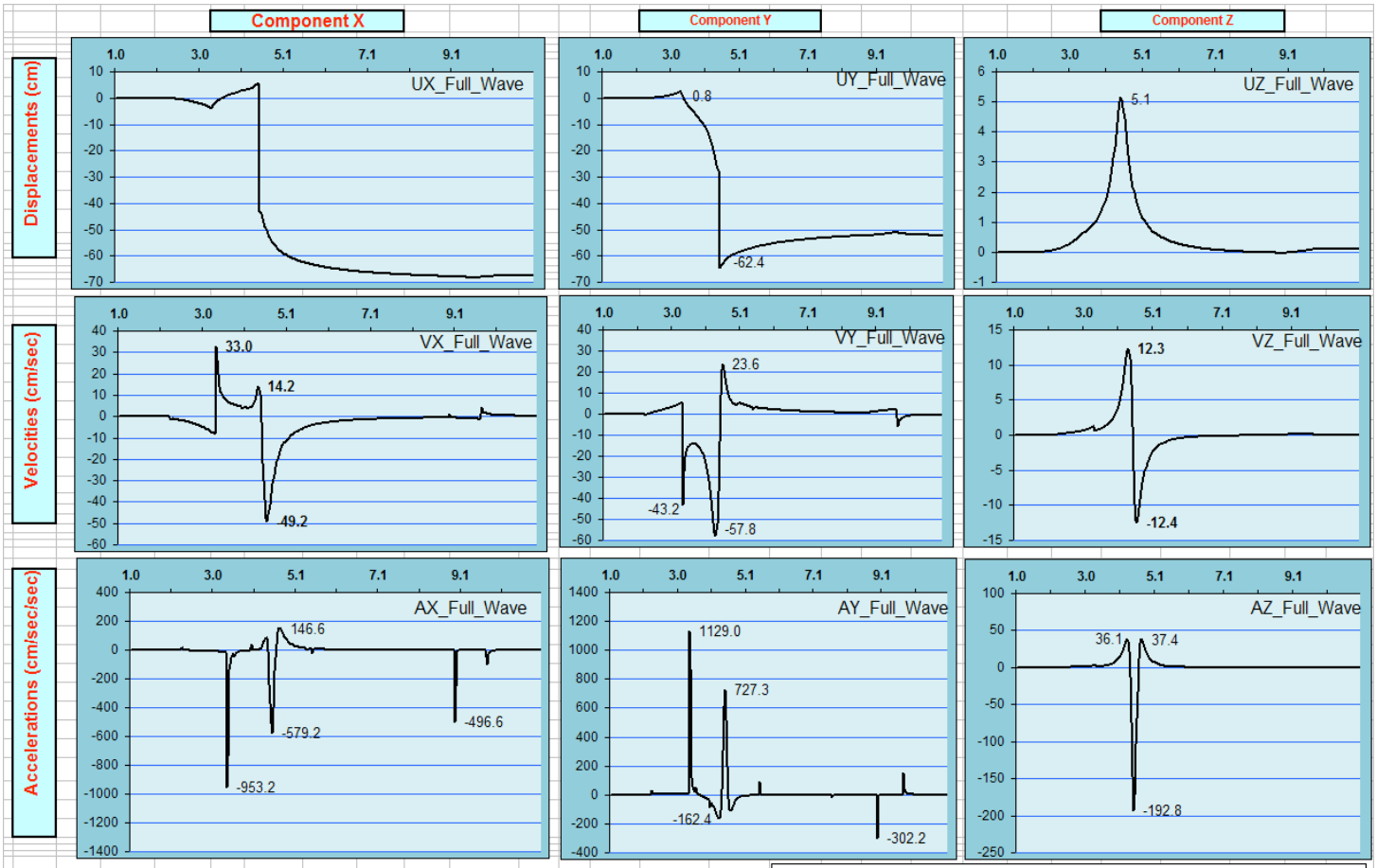

Max Velocities ~ 58 cm/sec **Max Accelerations ~ 1.13g**

All Points' coordinates are given in Left oriented coordinate system.
SHORELINE FAULT-8 SEGMENTS.Variant 6 as 1
Axes OX- East oriented Axes OY- South oriented Axes OZ- UP oriented.
Set of InPutData----------

Comment for Solve	Ground Motion Time Histories for Multisegment Fault Simulation using Bykovtsev's Methods													
Variant of Solve	**SHORELINE FAULT-8 SEGMENTS as 1 single_S1-S4 with uniform slip Bx=95cm**													
Velocities	**P- and S- wave**	in km/seconds				**6**	**4**							
Coordinates Station		**XN**	**YN**	**ZN**		in km	**-10.25**	**-8.66**	**-0.1**					
----------Rupture Parameters. It may be given for several SubFaults----														
Quantity of Sub-Fault is ----		**8**	**Record Start time sec=**	**1.0**	**Duration sec =**	**10.17**	**Quantity points =**	**300**	**Δt=**	**0.031**				

Ident Segment	**Star Time**	**Start Point Coordinate in km**			**Strike Angle**	**Dip Angle**	**Length**	**Width**	**Velocity**	**Dislocation Movement (in cm)**			**Distance Earth's surface to Rupture**	**Mo/μ = L*W*B**
	sec	**X0**	**Y0**	**Z0**	**grad**	**grad**	**km**	**km**	**km/sec**	**BX**	**BY**	**BZ**	**km**	
S1-1	**0**	**0**	**0**	**0**	**-142.6**	**0**	**0.3**	**15**	**3**	**95**	**0**	**0**	**0**	**0.004**
S1-2	**0.1**	**-0.238**	**-0.182**	**0**	**-142.6**	**0**	**0.3**	**15**	**3**	**95**	**0**	**0**	**0**	**0.004**
S1-3	**0.2**	**-0.476**	**-0.364**	**0**	**-142.6**	**0**	**0.3**	**15**	**3**	**95**	**0**	**0**	**0**	**0.004**
S1-4	**0.3**	**-0.714**	**-0.546**	**0**	**-142.6**	**0**	**1.5**	**15**	**3**	**95**	**0**	**0**	**0**	**0.021**
S1-5	**0.8**	**-1.904**	**-1.456**	**0**	**-142.6**	**0**	**4.76**	**15**	**3**	**95**	**0**	**0**	**0**	**0.068**
S2-3	**2.387**	**-5.69**	**-4.35**	**0**	**-142.6**	**0**	**7.89**	**15**	**3**	**95**	**0**	**0**	**0**	**0.112**
S3-5	**5.016**	**-11.95**	**-9.14**	**0**	**-142.6**	**0**	**3.78**	**15**	**3**	**95**	**0**	**0**	**0**	**0.054**
S5-4	**6.276**	**-14.96**	**-11.43**	**0**	**-142.6**	**0**	**3.64**	**15**	**3**	**95**	**0**	**0**	**0**	**0.052**
													Total	**0.320**

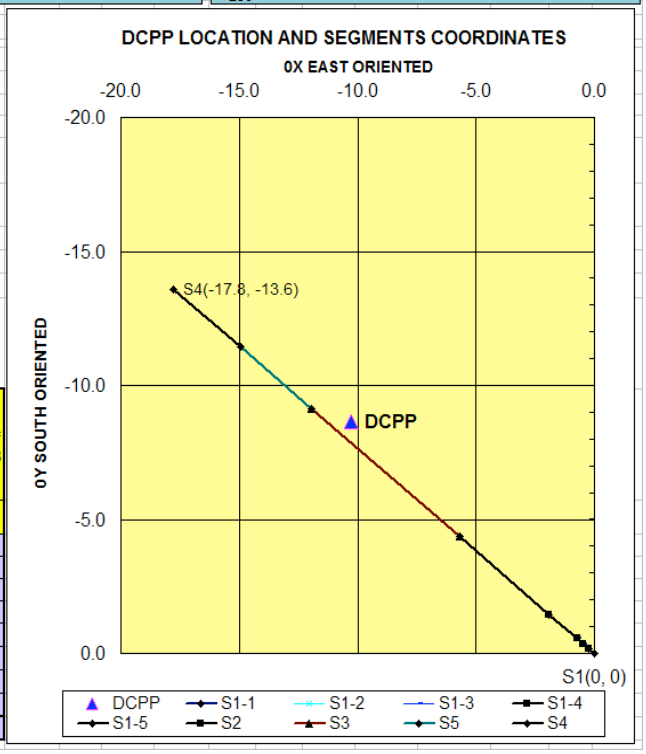

Fig. 2. Three-component LPSM for Shoreline Fault presented as 1 segment with uniform slip movement Bx=95cm.

The Non-uniform-slip or Variable Slip Simulations for SFZ presented as a Single Segment S1-S4 with Strike Angle -142.6^0.

The uniform-slip simulations for SFZ presented as a single segment S1-S4 are far away from reality. In order to simulate a more realistic kinematic source process we split first segment S1-S2 for 5 sub-segments and we assumed that for a rise time of 0.8 s average displacement on first segment reached 50 cm and then remain constant on first segment (Fig. 3), on the second segment S2-S3 average displacement jump up to 150 cm, and on third S3-S5 an fourth segment S5-S4 average displacement jump down up to 100cm and 87 cm, respectively. Results of simulated LPSM with effects of vibratory ground motion are presented on Fig. 3, and it is clear show that several large amplitude pulse-like velocity ground motions on components X and Y, and one pulse-like velocity motion observed on vertical Z component. Component X and component Y have a several strong maximum (>0.4g) in acceleration and component Z has only one maximum in acceleration. As we can see from Fig.3 for the non-uniform-slip simulations the maximum differences between maximum and minimum peak ground velocity (PGV) and peak ground acceleration (PGA) values for Y components (130 cm/s and 1.4g, respectively), and for vertical Z component the maximum differences between maximum and minimum PGV and PGA (39 cm/s and 0.36g, respectively). The first PGA~0.58g arrived at 3.4 sec, second PGA~0.5 arrived at 3.58 sec, third PGA~0.82g arrived at 3.98, and fourth PGA~1.16g arrived at 4.46 sec, and fifth PGA~0.42g arrived at 5.48 sec. Vertical motions in this case are approximately equal PGA~0.36g and arrived at 4.46 sec. Vertical PGV is approximately 30% to the maximum PGV for horizontal component Y for velocities, and approximately 31% to the maximum PGA horizontal component Y for acceleration.

Comparison Fig.2 and Fig.3 show that for uniform-slip we have only two PGA >0.4g acting during 2.5 second in time interval between 3sec and 5.5 sec, and for non-uniform-slip we have at least five PGA>0.4g. In case of non-uniform-slip (variable slip) movement on SFZ presented as a one segment we will have multiple seismic forces with PGA > 0.4g acting during 2.5 second in time interval between 3sec and 5.5 sec. LPSM with multiple oscillations have become a crucial consideration in SHA of DCPP due to cyclic load. The nature of such cyclic loading induces progressive alteration in the bearing capacity and may cause a "fatigue crack" in foundation and structure.

Recommendation # 2 for strike-slip with non-uniform movement on the SFZ. Based on obtained results for non-uniform-slip with variable movement, for structural design DCPP foundation and nonstructural elements at least 5-6 cyclic seismic loads with PGA>0.4g and acting during 2.5-3 sec should be taken in consideration for proper SHA. The total vector horizontal PGA for component X and Y for the maximum PGA arrived at 4.46 sec and may be estimated around 1.8g, and for vertical component Z maximum PGA arrived at 4.46 sec and may be estimated around 0.36 g. Vertical motions in this case are approximately equal 30.5% to the horizontal component Y for velocities, and approximately 20.4% to the horizontal component Y for acceleration.

The Non-uniform-slip or Variable Slip Simulations for SFZ presented as a Four Segments S1-S2, S2-S3, S3-S5 and S5-S4.

Figure 4 shows input data, SFZ configuration and results of simulation LPSM for North Segment S4 end point alternative with non-uniform (variable) slip movement Bx as presented on Fig.3. Real coordinates for segments S1-S2, S2-S3, S3-S5 and S5-S4 are presented in Table 1. Recalculated coordinates in global OXY coordinate system are presented in input data on Fig.4. The strike angles for segments S1-S2, S2-S3, S3-S5, and S5-S4, are -136.6^0, -150^0, -140.43^0, -140.84^0, respectively. The first segment S1-S2 split for 5 sub-segments and we assumed that for a rise time of 0.8 s average displacement on first segment reached 50 cm and then remain constant on first segment (Fig. 4), on the second segment S2-S3 average displacement jump up to 150 cm and we have a rupture twist approximately -13.0^0. On third segment S3-S5 – rupture twist approximately equal +10.0^0 and on fourth segment S5-S4 rupture twist approximately equal +0.5^0. The average displacements for third and fourth segments drop up to 100cm and 87 cm, respectively.

Results of simulated LPSM with effects of vibratory ground motion for twisting fault are presented on Fig. 4, and it is show that several large amplitude pulse-like velocity ground motions on components X and Y, and two pulse-like velocity motion observed on vertical Z component. Component X and component Y have a two strong maximum (PGA>0.4g) and a three strong maximum (PGA>1.1g) in acceleration and component Z has several maximum in acceleration also. As we can see from Fig.4 for twisting fault with non-uniform-slip simulations the maximum differences between maximum and minimum peak ground velocity (PGV) and peak ground acceleration (PGA) values for Y components (149 cm/s and 1.98g, respectively), and for vertical Z component the maximum differences between maximum and minimum PGV and PGA (36 cm/s and 0.31g, respectively). The first PGA~0.52g arrived at 3.44 sec, second PGA~0.7 arrived at 3.65 sec, third PGA~1.48g arrived at 3.98 sec, and fourth PGA~1.1g arrived at 4.46 sec, and fifth PGA~1.14g arrived at 5.48 sec. Vertical motions in this case are approximately equal PGA~0.31g and arrived at 4.46 sec. Vertical PGV is approximately 24% to the maximum PGV for horizontal component Y for velocities, and approximately 20% to the maximum PGA horizontal component Y for acceleration.

Comparison Fig.3 and Fig.4 show that in case of variable slip movement on SFZ presented as a one segment we will have multiple seismic forces with PGA > 0.4g acting during 2.5 second in time interval between 3sec and 5.5 sec with maximum PGA approximately equal 1.8g and average value of other four PGA approximately equal 0.6g. In case of twisted trajectory of segments

and the same variable slip movement on SFZ presented as a four segment we have increase in value of PGA. The maximum horizontal PGA arrived at 3.98sec and approximately equal 2.44g (increase in value 36%) and average value of other four PGA approximately equal 0.86g (increase in value 43%). Vertical motions in this case are approximately equal 30.5% to the maximum horizontal component Y for velocities, and approximately 20.4% to the maximum horizontal component Y for acceleration and have decrease in value 14%.

Recommendation # 3 for strike-slip with non-uniform movement and twisting segments on the SFZ. Based on obtained results for twisting fault and non-uniform-slip movement, for structural design DCPP foundation and nonstructural elements at least 5-6 cyclic seismic loads with PGA >0.4g and acting during 2.5-3 sec should be taken in consideration for proper SHA. The total vector for component X and Y for the maximum horizontal PGA forces may be estimated around 2.45g and arrived at 3.98 sec, and for vertical component Z maximum PGA around 0.31 g and arrived at 4.46 sec. Also, average value of other four horizontal PGA approximately equal 0.86g should be taken in consideration as cyclic load acting in interval approximately 3 sec.

The Non-uniform-slip Simulations for SFZ presented as a Six Segments S1-S2, S2-S3, S3-S5, S5-S4, and S3-S7, S7-S6.

Figure 5 give you an idea about input data, SFZ configuration and results of simulation LPSM for twisting at point S2 and branching in point S3 for North Segment S4 end point alternative and North Segment N40W fault alternative with non-uniform (variable) slip movement Bx as presented on Fig.3. Real coordinates for segments S1-S2, S2-S3, S3-S5, S5-S4, S3-S7, and S7-S6 are presented in Table 1. Recalculated coordinates in global OXY coordinate system are presented in input data on Fig.5. The strike angles for segments S1-S2, S2-S3, S3-S5, S5-S4, S3-S7, and S7-S6 are -136.6^0, -150^0, -140.43^0, -140.84^0, -134.3^0, -124.05^0, respectively. The first segment S1-S2 split for 5 sub-segments and we assumed that for a rise time of 0.8 s average displacement on first segment reached 50 cm and then remain constant on first segment (Fig. 5), on the second segment S2-S3 average displacement jump up to 150 cm and we have a rupture twist approximately -13.0^0. At point S3 fault trajectories have branching for North Segment S4 end point alternative and North Segment N40W fault alternative. For North Segment S4 end point alternative third segment S3-S5 – rupture twist approximately equal $+10.0^0$ and on fourth segment S5-S4 rupture twist approximately equal $+0.5^0$. The average displacements for third and fourth segments drop up to 50cm and 41 cm, respectively. For North Segment N40W fault alternative fifth segment S3-S7 rupture twist approximatle$+15.7^0$ and on fourth segment S5-S4 rupture twist approximately equal $+26.75^0$. The average displacements for S3-S7 and S7-S6 segments drop up to 50cm and 46 cm, respectively.
Results of simulated LPSM for twisted at point S2 and branching in point S3 fault are presented on Fig. 5, and it is show that several large amplitude pulse-like velocity ground motions on components X and Y, and two pulse-like velocity motion observed on vertical Z component. Component X and component Y have a several strong maximum with PGA>0.4g and a three very strong maximum with PGA>1.1g in acceleration and component Z has several maximum in acceleration also. As we can see from Fig.5 for twisting and branching fault with non-uniform-slip simulations the maximum differences between maximum and minimum peak ground velocity (PGV) and peak ground acceleration (PGA) values for Y components (146 cm/s and 1.87g, respectively), and for vertical Z component the maximum differences between maximum and minimum PGV and PGA (36.3 cm/s and 0.32g, respectively). The first PGA~0.48g arrived at 3.44 sec, second PGA~0.67 arrived at 3.65 sec, third PGA~1.41g arrived at 3.98 sec, and fourth PGA~1.1g arrived at 4.46 sec, and fifth PGA~1.05g arrived at 5.48 sec. Vertical motions in this case are approximately equal PGA~0.31g and arrived at 4.46 sec. Vertical PGV is approximately 24.9% to the maximum PGV for horizontal component Y for velocities, and approximately 17% to the maximum PGA horizontal component Y for acceleration.

Comparison Fig.3 and Fig.5 show that in case of variable slip movement on SFZ presented as a one segment we will have multiple seismic forces with PGA > 0.4g acting during 2.5 second in time interval between 3sec and 5.5 sec with maximum PGA approximately equal 1.8g and average value of other four PGA approximately equal 0.6g. In case of twisted and branching trajectory of segments and the same variable slip movement on SFZ presented as a four segment we have increase in value of PGA. The maximum horizontal PGA arrived at 3.98sec and approximately equal 2.31g (increase in value 28%) and average value of other four PGA approximately equal 0.81g (increase in value 35%). Vertical motions in this case are approximately equal 25% to the maximum horizontal component Y for velocities, and approximately 17.2% to the maximum horizontal component Y for acceleration and have decrease in value approximately 3%.

Recommendation # 4 for strike-slip with non-uniform movement and twisting and branching segments on the SFZ. Based on obtained results for twisting and branching fault and non-uniform-slip movement, for structural design DCPP foundation and nonstructural elements at least 5-6 cyclic seismic loads with PGA >0.4g and acting during 2.5-3 sec should be taken in consideration for proper SHA. The total vector for component X and Y for the maximum horizontal PGA forces may be estimated around 2.31g and arrived at 3.98 sec, and for vertical component Z maximum PGA around 0.31 g and arrived at 4.46 sec. Also, average value of other four horizontal PGA approximately equal 0.81g should be taken in consideration as cyclic load acting in interval approximately 3 sec.

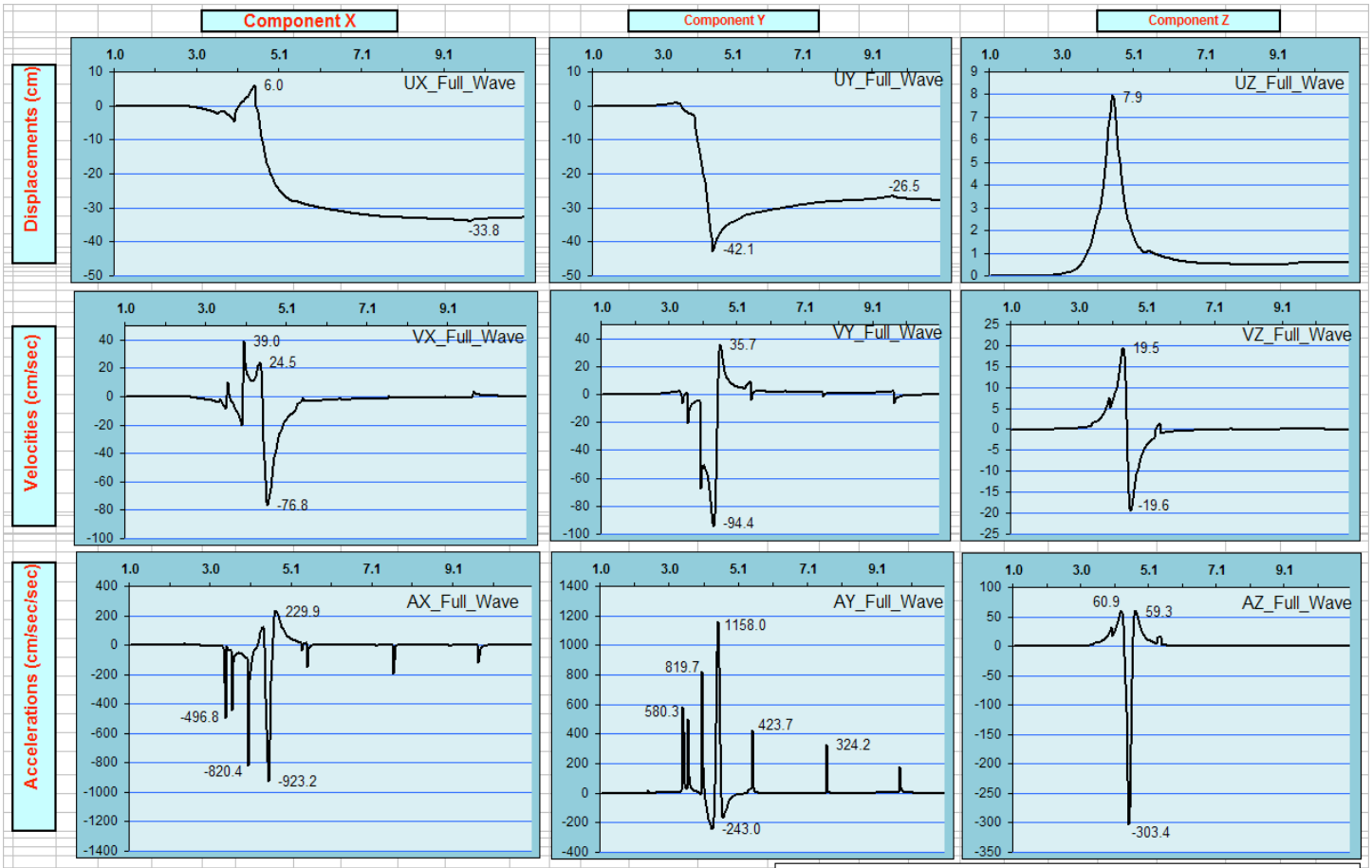

Max Velocities ~ 94.4 cm/sec Max Accelerations ~ 1.16g

All Points' coordinates are given in Left oriented coordinate system.
SHORELINE FAULT-8 SEGMENTS.Variant 8 as 1 (VARIABLE SLIP)
Axes OX- East oriented Axes OY- South oriented Axes OZ- UP oriented.
----------Set of InPutData----------

Comment for Solve	**Ground Motion Time Histories for Multisegment Fault Simulation using Bykovtsev's Methods**
Variant of Solve	**SHORELINE FAULT-8 SEGMENTS as 1 single_S1-S4 with variable slip Bx**

Velocities P- and S- wave	in km/seconds			**6**	**4**			
Coordinates Station	**XN**	**YN**	**ZN**		in km	-10.25	-8.66	-0.1

----------Rupture Parameters. It may be given for several SubFaults--

Quantity of Sub-Fault is ----				**8**	**Record Start time sec =**	**1**	**Duration sec =**	**10.17**	**Quantity points =**	**300**	**Δt=**	**0.031**	
Ident Segment	**Start Time**	**Start Point Coordinate in km**			**Strike Angle**	**Dip Angle**	**Length**	**Width**	**Velocity**	**Dislocation Movement (in cm)**			**Distance Earth's surface to Rupture**	**Mo/μ = L*W*B**
	sec	X0	Y0	Z0	grad	grad	km	km	km/sec	BX	BY	BZ	km	
S1-1	0	0	0	0	-142.6	0	0.3	15	3	1	0	0	0	0.0000
S1-2	0.1	-0.238	-0.182	0	-142.6	0	0.3	15	3	2	0	0.0	0	0.0001
S1-3	0.2	-0.476	-0.364	0	-142.6	0	0.3	15	3	4	0	0.0	0	0.0002
S1-4	0.3	-0.714	-0.546	0	-142.6	0	1.5	15	3	10	0	0.0	0	0.0023
S1-5	0.8	-1.904	-1.456	0	-142.6	0	4.76	15	3	50	0	0	0	0.0357
S2-3	2.387	-5.69	-4.35	0	-142.6	0	7.89	15	3	150	0	0	0	0.1775
S3-5	5.016	-11.95	-9.14	0	-142.6	0	3.78	15	3	100	0	0	0	0.0567
S5-4	6.276	-14.96	-11.43	0	-142.6	0	3.64	15	3	87	0	0	0	0.0475
0	0	0	0	0	0	0	0	0	0	0	0	0	Total	0.3200

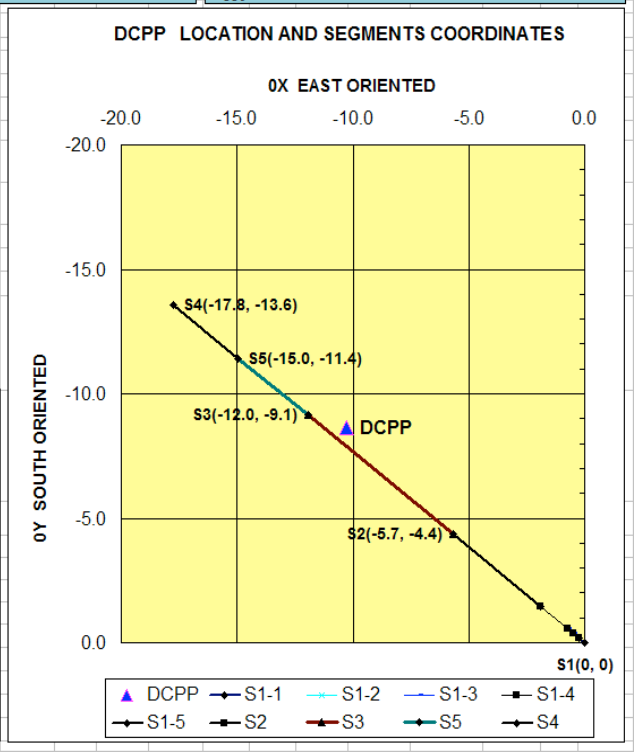

Fig. 3. Three-component LPSM for Shoreline Fault presented as 1 segment with variable slip movement Bx.

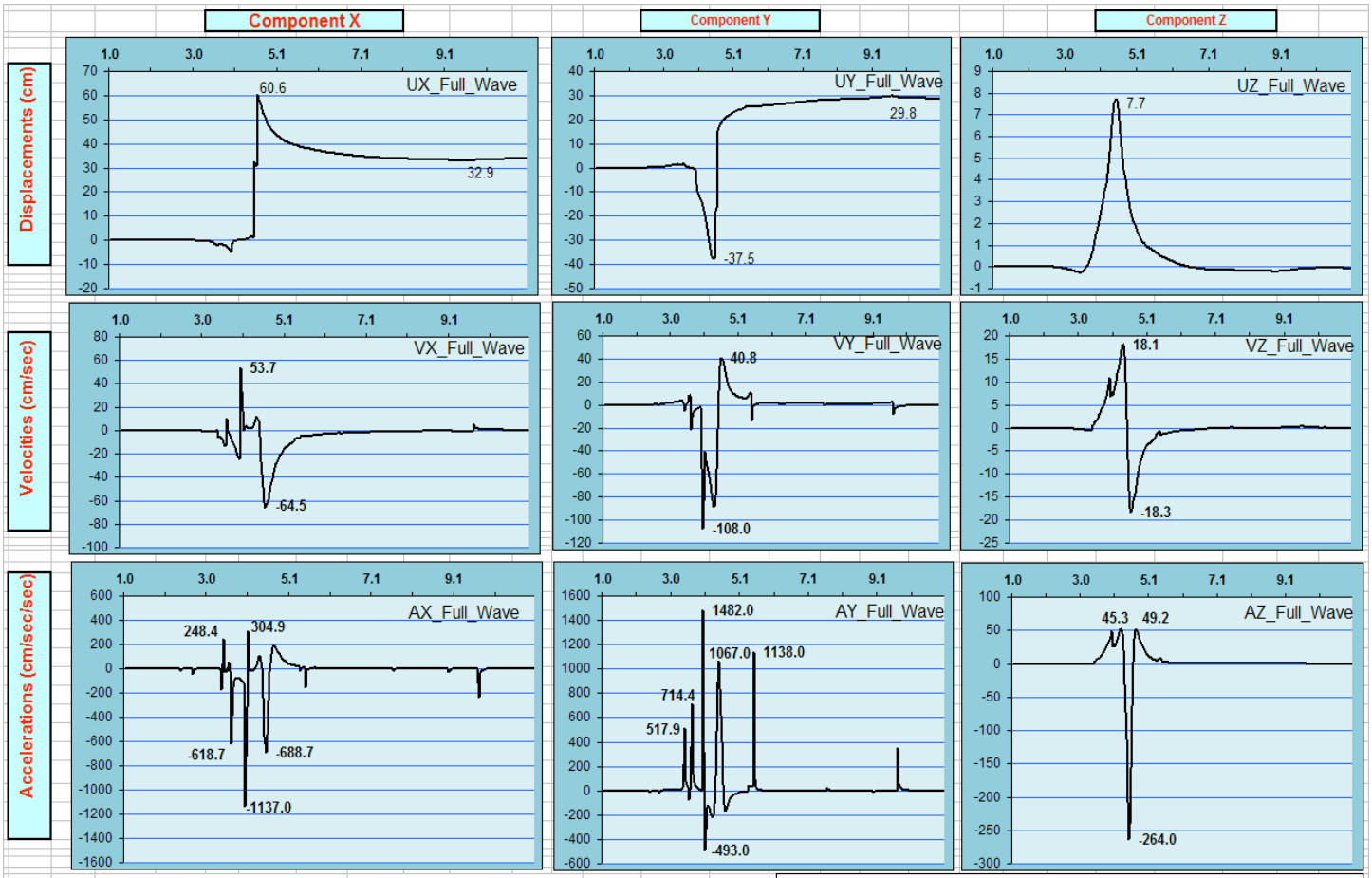

Max Velocities ~ -108 cm/sec **Max Accelerations ~ 1.48g**

All Points' coordinates are given in Left oriented coordinate system.
SHORELINE FAULT-8 SEGMENTS Variant-8 as 4 (VARIABLE SLIP).
Axes OX- East oriented Axes OY- South oriented Axes OZ- UP oriented.
Set of InPutData-------

Comment for Solve	**Ground Motion Time Histories for Multisegment Fault Simulation using Bykovtsev's Methods**
Variant of Solve	**SHORELINE FAULT-8 SEGMENTS as 4_S1-S2-S3-S5-4 with variable slip**

Velocities P- and S- wave	in km/seconds				**6**	**4**			
Coordinates Station	**XN**	**YN**	**ZN**		in km	-10.25	-8.66	-0.1	

----------Rupture Parameters. It may be given for several SubFaults----

Quantity of Sub-Fault is -----	**8**	**Record Start time sec =**	**1**	**Duration sec =**	**10.17**	**Quantity points =**	**300**	**Δt=**	**0.031**		

Ident Segment	**Start Time**	**Start Point Coordinate in km**			**Strike Angle**	**Dip Angle**	**Length**	**Width**	**Velocity**	**Dislocation Movement (in cm)**			**Distance Earth's surface to Rupture**	**Mo/μ = L*W*B**
	sec	X0	Y0	Z0	grad	grad	km	km	km/sec	BX	BY	BE	km	
S1-1	0	0	0	0	-136.6	0	0.3	15	3	1	0	0	0	0.0000
S1-2	0.1	-0.218	-0.21	0	-136.6	0	0.3	15	3	2	0	0	0	0.0001
S1-3	0.2	-0.436	-0.42	0	-136.6	0	0.3	15	3	4.0	0	0	0	0.0002
S1-4	0.3	-0.654	-0.63	0	-136.6	0	1.5	15	3	10	0	0	0	0.0023
S1-5	0.8	-1.526	-1.47	0	-136.6	0	4.76	15	3	50	0	0	0	0.0357
S2-3	2.387	-5.20	-4.93	0	-150.0	0	7.89	15	3	150	0	0	0	0.1775
S3-5	5.0167	-12.03	-8.87	0	-140.43	0	3.78	15	3	100	0	0	0	0.0567
S5-4	6.277	-14.94	-11.28	0	-140.84	0	3.64	15	3	87	0	0	0	0.0475
													Total	0.3200

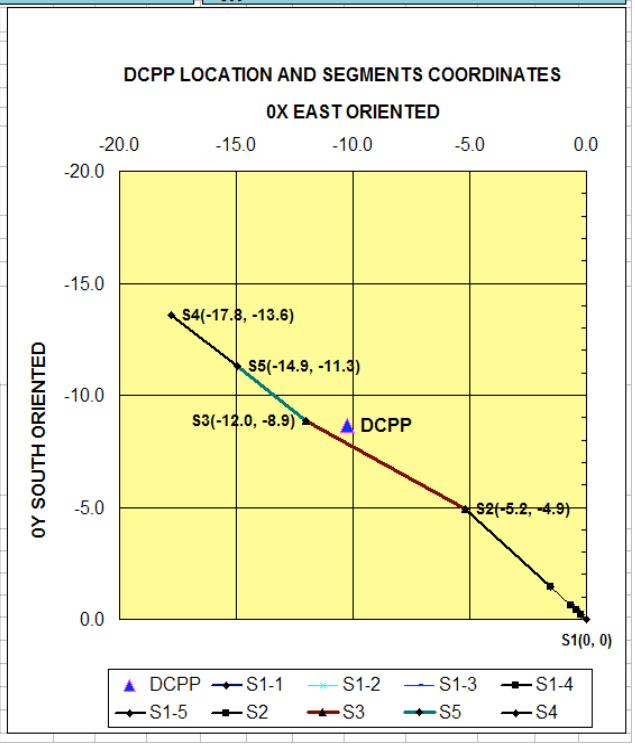

Fig. 4. Three-component LPSM for Shoreline Fault presented as 4 twisting segments with variable slip movement Bx.

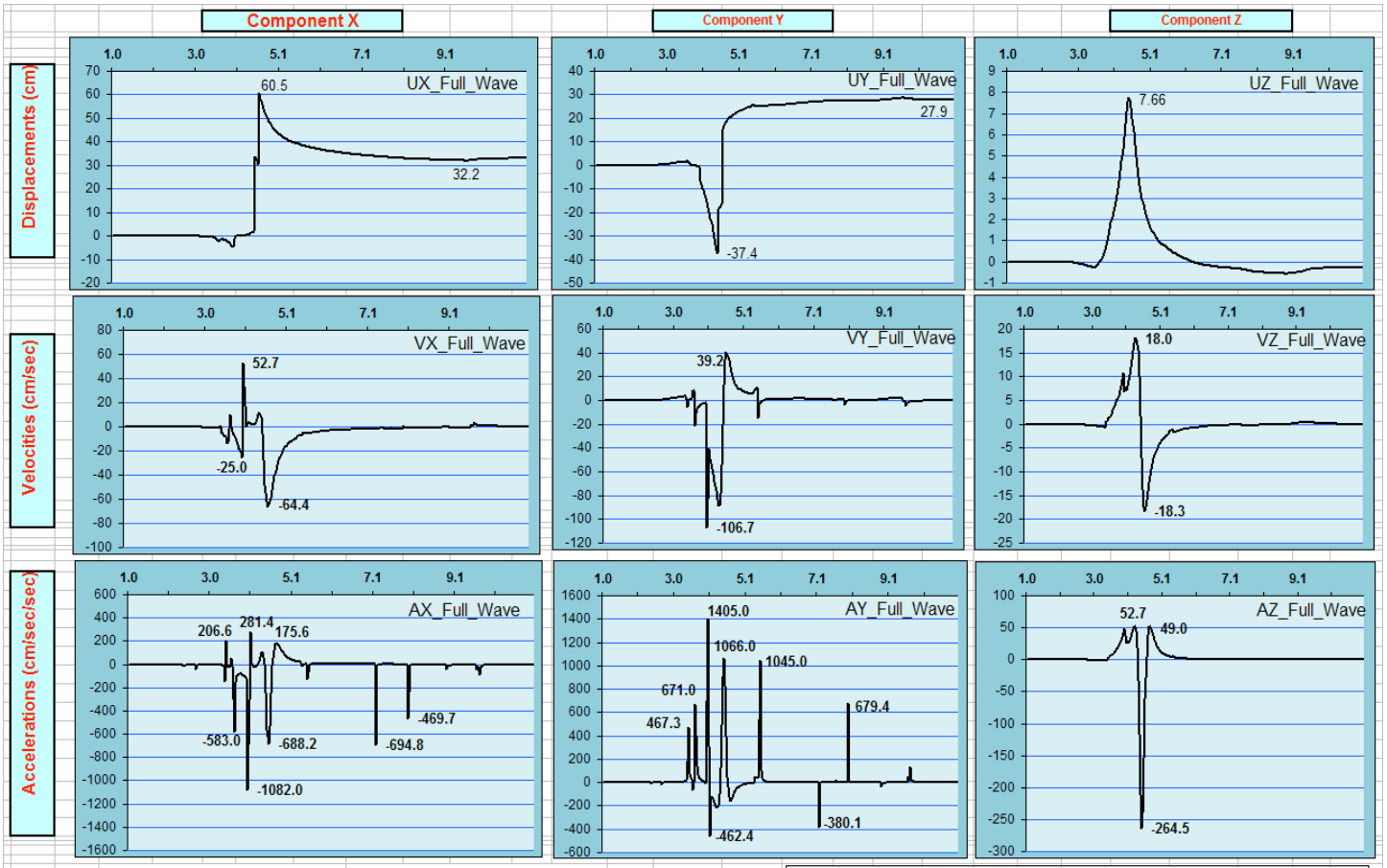

Max Velocities ~ 107 cm/sec **Max Accelerations ~ 1.41g**

All Points' coordinates are given in Left oriented coordinate system.
SHORELINE FAULT-10 SEGMENTS Variant-10 as 6-BRANCHING SEGMENTS.
Axes OX- East oriented Axes OY- South oriented Axes OZ- UP oriented.
Set of InPutData----------

Comment for Solve	**Ground Motion Time Histories for Multisegment Fault Simulation using Bykovtsev's Methods**
Variant of Solve	**SHORELINE FAULT-10 SEGMENTS as 6 S1-S2-S3-S5-S4-S7-S6 with branching segments and variable slip**

Velocities P- and S- wave	in km/seconds			**6**	**4**			
Coordinates Station	**XN**	**YN**	**ZN**	in km	**-10.25**	**-8.66**	**-0.1**	

----------Rupture Parameters. It may be given for several SubFaults--------

Quantity of Sub-Fault is --	**10**	**Record Start time sec =**	**1**	**Duration sec =**	**10.17**	**Quantity points =**	**300**	**Δt=**	**0.031**				
Ident Segment	**Start Time**	**Start Point Coordinate in km**			**Strike Angle**	**Dip Angle**	**Length**	**Width**	**Velocity**	**Dislocation Movement (in cm)**			**Distance Earth's surface to Rupture**	**Mo/μ = L*W*B**
	sec	X0	Y0	Z0	grad	grad	km	km	km/sec	BX	BY	BZ	km	
S1-1	0	0	0	0	-136.6	0	0.3	15	3	1	0	0	0	0.0000
S1-2	0.1	-0.218	-0.21	0	-136.6	0	0.3	15	3	2.0	0	0	0	0.0001
S1-3	0.2	-0.436	-0.42	0	-136.6	0	0.3	15	3	4.0	0	0	0	0.0002
S1-4	0.3	-0.654	-0.63	0	-136.6	0	1.5	15	3	10	0	0	0	0.0023
S1-5	0.8	-1.526	-1.47	0	-136.6	0	4.76	15	3	50	0	0	0	0.0357
S2-3	2.387	-5.20	-4.93	0	-150.0	0	7.89	15	3	150	0	0	0	0.1775
S3-5	5.016	-12.03	-8.87	0	-140.43	0	3.78	15	3	50	0	0	0	0.0284
S5-4	6.277	-14.94	-11.28	0	-140.84	0	3.64	15	3	41	0	0	0	0.0224
S3-7	5.016	-12.03	-8.88	0	-134.3	0	4.44	15	3	50	0	0	0	0.0333
S7-6	6.497	-15.13	-12.05	0	-124.25	0	2.92	15	3	46	0	0	0	0.0201
													Total	**0.3200**

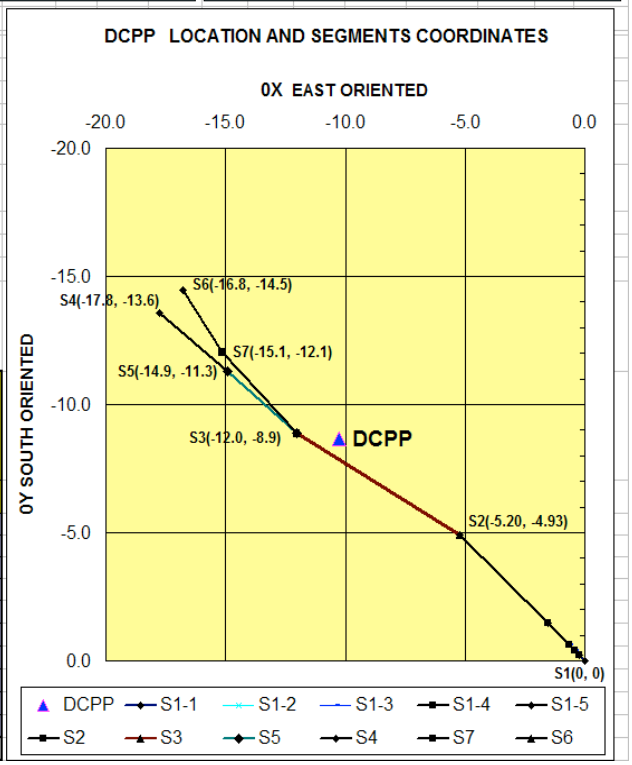

Fig. 5. Three-component LPSM for Shoreline Fault presented as 6 twisting and branching segments with variable slip movement Bx.

CONCLUSIONS

In this paper we performed a simulation study for the DCPP site with estimating effect of Shoreline Fault Zone (SFZ) segmentations on simulation of long-period seismic motions (LPSM) and seismic load. Four different scenarios of possible seismic sources acting in SFZ are presented in Fig. 2 – Fig. 5 with effects of vibratory ground motion. As a result of presented analysis it is possible to conclude, that for DCPP site LPSM may contain pulses with multiple oscillations (due to SFZ segmentation) which can cause severe nonlinear structural response. LPSM with multiple oscillations have become a crucial consideration in SHA of DCPP. The **segmentations** of SFZ introduce additional **extremes** for LPSM **and effects of vibratory ground motion should be properly estimated in SHA and included in design of seismic load for DCPP.** These findings including the shape, amplitude and duration of LPSM on the DCPP site location in relation to the SFZ, main rupture orientation, complexity of rupture on each segment, and mutual arrangement of subsources shall be investigated more accurate for proper seismic hazard assessment DCPP. We not recommended using in the future scaling approach for DCPP due to differences in fault segmentations for different faults and sites locations. For proper and more accurate analysis we recommend to use deterministically simulated seismic sources time histories and time-domain procedures that are one of more effective method for proper estimate the effects of vibratory ground motion and several cyclic load on DCPP foundation and non-structural elements.

The strike-slip fault simulations also show that seismic hazard to DCPP structures from both horizontal and vertical component in the near-fault distance range, significant differential motions can be expected over the length of building foundations, particularly for SFZ segments that come close to the DCPP. As Figures 2-5 show, the acceleration and velocity records are significantly more complex than displacement records. Maximum amplitudes of acceleration as well as the least duration are observed for SFZ with twisting (Fig.4) and twisting and branching scenarios presented on Fig.5.

In addition, SFZ variations in fault segmentation geometry can introduce additional complexity that can affect the level of seismic loads and time period of different PGA. Based on the results of this study, DCPP located very close to twisted segment and LPSM with both total horizontal (Component X plus Component Y) and vertical Component Z would be subjected to contributions from the respective SFZ segments. While this study points out general behaviors of LPSM for only strike slip movement on each segment in the very near-fault distance range, future work must investigate the effects of different sources of rupture complexity on each segment of SFZ and the effects of this on both total horizontal and vertical motions for DCPP.

Finally, the simulations presented in this paper only account strike-slip motion on four segments of SFZ and not included in consideration possible dip-slip motions from seismic sources located inside the San Luis Bay fault zone which also lies closest to the DCPP and has the cumulative **rate of vertical separation** about 0.14 mm/yr. Considering the effect of segmentations located inside the San Luis Bay fault zone together with segmentation of Shoreline fault zone with different faulting style should be investigated in the future using the 3-D method summarized here.

The emergency in Japan (March 2011) provides as an important wake-up call for contribution our tools and knowledge for the proper seismic hazard analysis nuclear plants located in California, and we cannot afford to ignore it. We have concerns about seismic issues at DCPP and proper estimate of ground motions. DCPP has submitted its application to the NRC for license renewal. The 3-D seismic studies including deterministic simulated ground motion records for displacement, velocity and acceleration from different seismic sources need to be considered as part of the license renewal process at DCPP and should also be part of the NRC's review of DCPP license renewal application.

REFERENCES

Bykovtsev, A. S. [1986a], "Propagation of Complex Discontinuities with Piecewise Constant and Variable Velocities along Curvilinear and Branching Trajectories", *Appl. Math. Mech.(PMM)* Vol. 50, No. 5, pp. 620-628.

Bykovtsev, A. S. [1986b], "Modeling of Fracture Processes Occurring in the Focal Zone of a Tectonic Earthquake", *Proc. Intern. Conf. on Computational Mechanics*, 25-29 May, Tokyo, Springer-Verlag. Vol.1. Ed.: G. Yagawa, S. N. Atluri, III-221-226.

Bykovtsev, A. S. and D.B. Kramarovskii [1986], "Displacement Field Produced by a Propagating Rectangular Rupture Plane: Exact Three-dimensional Solution", *Proc. Intern. Conf. on Computational Mechanics*, 25-29 May, Tokyo, Springer-Verlag. 25-29 May, Tokyo, Springer-Verlag. Vol..*2*. Ed.: G. Yagawa, S. N. Atluri, *VI-315-320*.

Bykovtsev, A. S. and D.B. Kramarovskii [1987], "On the Propagations of a Complex Fracture Area, Exact Three-dimensional Solution", *Appl. Math. Mech.(PMM) Vol.* 51, No. 1, pp. 89-98.

Bykovtsev, A. S. and D.B. Kramarovskii [1989], "Non-Stationary Supersonic Motion of a Complex Discontinuity", *Appl. Math. Mech.(PMM)* Vol. 53, No. 6, pp. 779-786.

Bykovtsev, A.S**.**, and V.Yu. Sokolov, [1989], "Numerical Simulation of the Wave Field in the Near Zone of a Step-Like Propagating Curvilinear Fault and Analysis of High-Frequency Radiation", *Izv. An. SSSR Fiz. Zem*. No. 3, pp. 3-16.

Bykovtsev, A.S., and V.Yu. Sokolov, [1990], "Numerical simulation of wave fields and seismic intensity patterns in earthquake near-field zones*"*, *Acta Geophys. Pol*. No. 38, pp. 111-133.

Bykovtsev, A.S., Prokhorenko G.A., and V. N. Sytenkov, [2000], "Analyses of Geodynamic and Seismic Processes at Development of Deposits". *Navoi Mining and Metallurgical Works, Zerafshan, Uzbekistan,* 266 pp.

Bykovtsev, A. S. [2009a], "Deterministic Simulated Ground Motion Records under ASCE/SEI 7-05: Guidance For The Geotechnical Industry", *Report of the Regional Academy of Natural Sciences,* 2009 for Invited presentation on Seismological Society of America Annual Meeting, 8-10 April, Monterey, California, 14 pages.

Bykovtsev, A. S. [2009b], "Analytical review of presentations at Special Session "Deterministic Simulated Ground-Motion Records under ASCE/SEI 7-05: Guidance for the Geotechnical Industry" with Summary, Conclusions and Recommendations". *Report of the Regional Academy of Natural Sciences, 3 May,* 2009. Project #BAS-013-03, 23pp.

Bykovtsev, A. S. [2009c], "Meeting of the ASCE -7-05 Seismic Subcommittee "Minimum Design Loads for Buildings and Other Structures" San Francisco - August 21-22, 2009. PROPOSAL FOR CHANGE: ASCE 7-05 Section 21.1.1 Base Ground Motions Submitted by Dr. Alexander Bykovtsev, Ph.D., P.E., M.ASCE. *Report of the Regional Academy of Natural Sciences, for Oral Presentation on the Meeting of the ASCE -7-05 Seismic Subcommittee,* 21 August, 2009, Project No BAS-013-08, 10 pages.

Bykovtsev, A.S., and M. Kasimov [2009], "Site Specific Investigation for National Bank of Uzbekistan with Time History Analyses of Simulated Ground Motion", *Report of the Regional Academy of Natural Sciences, 2009 for Invited presentation on Seismological Society of America Annual Meeting,* 8-10 April, Monterey, California, *32* pages.

Bykovtsev A.S. [2011], "Preliminary simulation of long-period seismic motions and seismic load for Shoreline fault zone segmentations in area of Diablo Canyon Power Plant", *Report of the Regional Academy of Natural Sciences prepared for presentation on 4th IASPEI / IAEE International Symposium Effect of Surface Geology on Seismic Motion* April 25, 2011, (24 pages).

Graizer, V., and E. Kalkan [2007], "Ground motion attenuation model for peak horizontal acceleration from shallow crustal eartquakes", *Earthquake Spectra, Vol. 23, No 3, pp. 585-613.*

Hanson, K.L., W.R. Lettis, M.K. McLaren, W.U. Savage, and N.T. Hall [2004], "Style and rate of Quaternary deformation of the Hosgri fault zone, offshore south-central California, in Evolution of Sedimentary Basins/Offshore Oil and Gas Investigations—Santa Maria Province, Keller, M.A. (Editor)", *U.S. Geol. Surv. Bull. 1995-BB*, 33 pages.

Hardebeck, J.L. [2010], "Seismotectonics and Fault Structure of the California Central Coast" *Bull. Seismol. Soc. Am.* Vol. 100, No.3, pp. 1031-1050.

Leonard, M. [2010], "Earthquake Fault Scaling: Self-Consistent Relating of Rupture Length, Width, Average Displacement, and Moment Release" *Bull. Seismol. Soc. Am.* Vol. 100, No. 5A, pp.1971-1988.

Lettis, W.R. and N.T. Hall [1994], "Los Osos fault zone, San Luis Obispo County, California, in Seismotectonics of the Central California Coast Ranges", Alterman, I.B., R.B. McMullen, L.S. Cluff, and D.B. Slemmons (Editors), *Geol. Soc.Am. Special Paper 292*, pp. 73-102.

McLaren, M.K. and W.U. Savage [2001], "Seismicity of South-central Coastal California: October 1987 through January 1997", *Bull. Seismol. Soc. Am. Vol.* **91**, pp. 1629-1658.

Pacific Gas and Electric Company (PG&E) [2011], "Report on the Analysis of the Shoreline Fault Zone, Central Coastal California", *Report to the U.S. Nuclear Regulatory Commission* , January 2011.

Pacific Gas and Electric Company (PG&E) [2010]. Progress Report on the Analysis of the Shoreline fault zone, central coast California, Enclosure 1, *PG&E Letter DCL-10-003*, January 2010.